A Multi-Distribution Network Calculation and Control Method Based on Voltage-Sensitive Load

Pu Hua, Cuihua Tian, Xuzhe Li, Hang Zhou, Kunquan Bao and Jiaxin Yuan
State Key Laboratory of Power Grid Environmental Protection, School of Electrical Engineering and Automation
Wuhan University
Wuhan 430072, China
huapuu@whu.edu.cn

***Abstract*—With increasing renewable energy penetration, active power accommodation and voltage violations have become critical challenges in modern power grids. Although Conservation Voltage Reduction (CVR)-based voltage-sensitive load control is effective in individual distribution networks or microgrids, extending it to multi-distribution networks (MDNs) is challenging due to large-scale topology and power flow coupling. This paper presents a unified calculation and control framework for centralized voltage-sensitive load dispatch in MDN. A linear power flow-based aggregation method and a Wirtinger-calculus-based calculation model are developed to enable scalable and consistent dispatch. Case studies on a practical MDN in Hangzhou, China, show that the proposed framework reduces total operating costs, improves voltage compliance, and remains computationally tractable.**

***Index Terms*--Linear power flow; multi-distribution network; voltage-sensitive load, Wirtinger calculus.**

I. Introduction

As more renewable energy resources (RESs) are integrated into the power system, both supply and demand exhibit significant uncertainty 0. In this context, it is urgent to leverage flexibility resources not only on the supply side but also on the demand side.

On the supply side, various converter-based strategies have been studied due to their ability to regulate both active and reactive power. However, methods for controlling DER power curtail the output of DERs and reduce the economic efficiency of DERs. Consequently, researchers have proposed many innovative regulation strategies that consider energy storage systems (ESSs). These aforementioned studies focus on the collaboration of resources on both the supply and storage sides, lacking the participation of the demand side resources.

On the demand side, flexibility can be broadly categorized into demand response (DR) and direct load control (DLC). DR incentivizes customers to shift or curtail consumption through prices or rewards, but its response is typically slow, making it less suitable for fast-timescale regulation. In contrast, DLC can accurately achieve applications on different time scales such as peak shaving and frequency modulation by controlling the load process 0, load switching 0, and load voltage 0. Among these options, load process control relies on specific temperature systems or industrial processes, resulting in limited applicability. Load switching control is discrete control and may disrupt customer behavior.

In comparison, load voltage control regulates load power through Var/Volt control, enabling fast and continuous response with low implementation cost. This approach relies on the voltage sensitivity of loads, which are commonly modeled using the ZIP load model consisting of constant impedance (Z), constant current (I), and constant power (P) components [5]. Exploiting these voltage-dependent load characteristics, Conservation Voltage Reduction (CVR) has emerged as a representative load voltage control strategy. Recent studies have demonstrated the effectiveness of voltage-sensitive load control in frequency regulation, including applications in Smart Transformer-based systems [6] and isolated microgrids with droop control [7].

However, most of the above studies are carried out in a single distribution network or under simplified power flow scenarios, where the interactions among distribution networks through the transmission network are neglected. In a multi-distribution network (MDN) scenario, the coupling effects through transmission networks introduce several challenges: (1) voltage regulation in one distribution network affects the power balance and voltage profiles of adjacent networks; (2) the slack bus voltage is no longer fixed but varies with the overall system state; (3) MDNs contain numerous ZIP loads and controls, imposing heavy computational burdens. These limitations highlight the need for a unified MDN calculation framework that captures the inter-network interactions while maintaining computational tractability.

Therefore, to enable accurate and efficient centralized dispatch of voltage-sensitive loads in MDNs, this paper proposes an MDN-oriented calculation and control method. The key contributions of this work are summarized as follows:

- A distribution network equivalent load aggregation method based on linear power flow modeling is developed, which enables scalable representation of

This work was supported by the National Natural Science Foundation of China under Grant 52577177, 52207182 and U2166207.

979-8-3315-8138-1

voltage-sensitive loads while preserving feeder losses and mixed ZIP characteristics.

- A Wirtinger-calculus-based MDN calculation and dispatch framework is proposed, enabling consistent power–voltage evaluation and coordinated dispatch without repeated Jacobian inversions.
- The proposed method is validated on a practical MDN in Hangzhou, China. The results demonstrate that incorporating voltage-sensitive loads into centralized dispatch reduces total operating costs, improves voltage compliance, and highlights the value of coordinated active/reactive regulation.

II. Distribution Network Calculation Method

A. *Equivalent Load Calculation Method for Distribution Network Based on Linear Power Flow*

To reduce the number of system nodes, it is necessary to equate the loads in distribution network to a substation equivalent load connected to the 10-kV bus of the substation. According to the implicit Zbus Gauss method, the voltage of distribution network U_L can be expressed as follows:

$$U_L = -Y_{LL}^{-1} Y_{L0} U_0 + Y_{LL}^{-1} I_L \tag{1}$$

Where, Y_{L0} is the mutual admittance matrix between the head-end node and the remaining nodes, Y_{LL} is the node admittance matrix between the remaining nodes, U_0 is the voltage of slack node, and I_L is the current of distribution network. The current of ZIP loads I_L can be expressed as:

$$I_L = Y_{eq}^* U_L + I_s^* + \frac{S_{pq}^*}{U_L^*} \tag{2}$$

Where, Y_{eq}, I_s, S_{pq} represent the constant impedance, constant current and constant power component of the load, respectively. The symbol (*) represents the complex conjugate. The constant power component forms a nonlinear relationship and can be equivalently linearized by geometric series as 0:

$$I_L = (Y_{eq}^* - S_{pq}^*) U_L + (I_s^* + 2S_{pq}^*) \tag{3}$$

The slope and constant term of (3) are denoted by k_1 and b_1, respectively. After adopting the generator reference direction, we substitute them into (1) to obtain:

$$U_L = -(\mathrm{diag}(k_1) + Y_{LL})^{-1} (Y_{L0} U_0 + b_1) \tag{4}$$

The slope and constant term of (4) are denoted by k_2 and b_2, respectively. Furthermore, the relationship between load power and voltage can be approximated as linear by conservation voltage reduction factor (CVR_f) :

$$S_L = CVR_f (|U_L| - 1) + S_0 \tag{5}$$

Where, S_0 represents the nominal power of the loads, S_L represents the actual power of the loads, and CVR_f is the CVR factor for loads. This factor is defined as the percentage change in load power corresponding to a 1% change in voltage 0.

Rearranging (4)–(5), it follows that, for any node in the distribution network, its load can be represented as an equivalent load referred to the slack bus. The CVR_f of loads remains unchanged, while the power becomes k_2 times the original value, with an additional constant power load of $b_2 CVR_f$.

B. *Calculation Model in MDN Based on Wirtinger Calculus*

In traditional power system analysis, the Jacobian matrix J and its inverse are widely used for sensitivity analysis in the power system. This method is more applicable to the system under small-signal perturbations. In MDN systems, the large number of nodes leads to high computational complexity in matrix inversion. Moreover, Jacobian-based analytical methods suffer from large errors and high computational burden in large-scale MDN applications. Therefore, an MDN calculation model based on Wirtinger calculus is proposed. By converting the voltage from polar coordinates to algebraic form for calculation, the matrix becomes more compact without increasing the matrix complexity. In addition, the proposed approach only requires factorizing the Ybus, which can be reused as long as the network topology remains unchanged. For an n-node system, the power injection S_i at bus i can be expressed by Wirtinger calculus as 0:

$$S_i = U_i \sum_{m=1}^{n} (Y_{im} U_m)^* \tag{6}$$

$$\Delta S = \mathrm{diag}(I^*) \Delta U + \mathrm{diag}(U) Y^* \Delta U^* \tag{7}$$

In the following, the coefficients associated with ΔU and ΔU^* in (7) are denoted by H_1 and K_1, respectively. The power of loads in MDN could be expressed as:

$$\Delta S_{\mathrm{Load}} = -\mathrm{diag}(Y_{eq} \circ U^* + I_s) \Delta U - \mathrm{diag}(Y_{eq} \circ U) \Delta U^* \tag{8}$$

Where, the symbol (○) represents Hadamard product. After obtaining the power-voltage relationship in the power grid and the load, it is necessary to establish a transfer function matrix model based on Wirtinger calculus to solve the iterative solution between power and voltage. The closed-loop response model of the system is composed of the open-loop models of the load and the power grid in (7) and (8). After expanding the power part, the schematic diagram of its transfer function model is shown in Fig. 1.

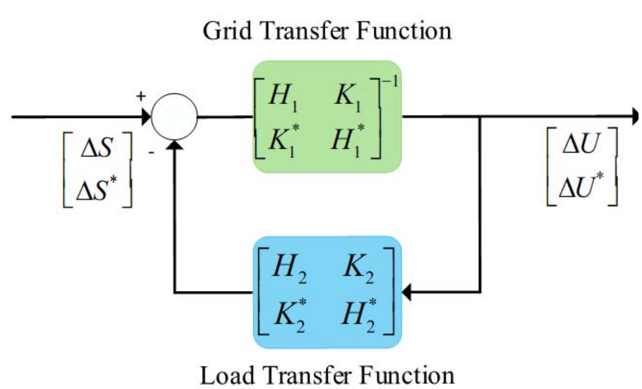

Figure 1. Extended Closed-loop Transfer Function Diagram

According to transfer function theory, the power-voltage relationship considering power grid power flow and load ZIP characteristics can be expressed as:

$$\begin{bmatrix} \Delta S \\ \Delta S^* \end{bmatrix} = \begin{bmatrix} H_1 + H_2 & K_1 + K_2 \\ (K_1 + K_2)^* & (H_1 + H_2)^* \end{bmatrix} \begin{bmatrix} \Delta U \\ \Delta U^* \end{bmatrix} \tag{9}$$

III. Voltage-Sensitive Load Control Model for MDN

A. Modeling of Adjustable Equipment

1) Converters

For any converter, the output power must satisfy the converter capacity and power factor constraints:

$$P_{\text{con}}^2 + Q_{\text{con}}^2 \le S_{\text{con,max}}^2 \tag{10}$$

$$|P_{\text{con}}|/S_{\text{con}} \ge 0.95 \tag{11}$$

Where, P_{con}, Q_{con} and S_{con} represent the active, reactive and apparent power of converter, respectively. $S_{\text{con,max}}$ represents the maximum apparent power of the converter.

Converters can be divided into grid-following (GFL) converters and grid-forming (GFM) converters according to different control methods. From the perspective of operating characteristics, GFL converters can be equivalent to a variable current source with parallel high impedance, and control power by controlling current output. The reactive output can be freely adjusted. To reduce the wind and solar curtailment rate, the active output of power-type converters generally operates in the Maximum Power Point Tracking (MPPT) mode and limited capability for active power regulation.

Different from GFL converters, the equivalent model of GFM converters is a variable voltage source with series low impedance, which controls power through voltage control. Such converters cannot only directly control the output power by actively controlling the power reference P_{ref} and Q_{ref}, but also automatically control the power through GFM control strategies. This paper takes droop control as an example to analyze the operating characteristics of GFM converters. Its P-f and Q-V droop equations are shown in (12)-(13):

$$\omega = \omega_{\text{ref}} - D_p (P_{\text{ref}} - P_{\text{con}}) \tag{12}$$

$$E = E_{\text{ref}} - D_q (Q_{\text{ref}} - Q_{\text{con}}) \tag{13}$$

Where, ω and E are the frequency and voltage of the converter, D_p and D_q are the droop coefficients of the converter, and ω_{ref}, E_{ref}, P_{ref}, Q_{ref} are the frequency, voltage, active and reactive reference values controlled by the converter. The MDN is a stable grid, ω and ω_{ref} are fixed at 50Hz(or 60Hz), and the other reference values are controllable.

For ESS converter, its state of charge (SoC) needs to be considered. Let the operation time t and the initial SoC SoC_0, its active output should satisfy:

$$P_{\text{dis}} \le \frac{(SoC_0 - SoC_{\min}) S_{\text{ESS}} \eta_{\text{dis}}}{t} \tag{14}$$

$$-P_{\text{cha}} \le \frac{(SoC_{\max} - SoC_0) S_{\text{ESS}}}{\eta_{\text{cha}} t} \tag{15}$$

Where, P_{dis}, P_{cha} represent the discharge and charge power of ESS, respectively, η_{dis}, η_{cha} represent the discharge and charge efficiency of ESS, respectively, $SoC_{\min}$, $SoC_{\max}$ represent the minimum and maximum SoC of ESS, respectively.

2) Dynamic Reactive Power Compensation Equipment

In high-voltage MDN, dynamic reactive compensation equipment is typically implemented using power-electronic-based STATCOM or electromagnetic-type magnetically controlled reactor (MCR), which are suitable for operation at higher voltage levels 0-0. This paper takes the MCR as the research object of dynamic reactive power compensation equipment.

To increase the utilization rate and flexibility of MCR, it is often operated in parallel with switched capacitors of the same capacity to realize continuous adjustment of compensation power from inductive to capacitive. Therefore, the reactive power constraint of MCR Q_G is shown in (16):

$$-Q_{\text{mcr,max}} \le Q_G \le Q_{\text{mcr,max}} \tag{16}$$

Where, $Q_{\text{mcr,max}}$ represents the capacity of the magnetically controlled reactor.

B. The Optimization Model

1) Objective Function

The objective is to minimize the operating cost while satisfying frequency- and voltage-related requirements. The economic optimization objective can be expressed as:

$$\begin{aligned} \min C_{\text{eco}} = & \sum_{p=1}^{n_{\text{PV}}} c_{\text{cur}} \min(\Delta P_p^{\text{PV}}, 0)^2 + \sum_{q=1}^{n_{\text{ESS}}} c_{\text{cha/dis}} |\Delta P_q^{\text{ESS}}|^2 \\ & + \sum_{r=1}^{n_{\text{PV}}+n_{\text{ESS}}} c_{\text{con}} \left| \frac{\Delta Q_r}{S_{\text{con,max}}} \right| + \sum_{s=1}^{n_{\text{Line}}} c_r \Delta P_r^{\text{Line}} \end{aligned} \tag{17}$$

Where, c_{cur} represents the curtailment cost of PV, $c_{\text{cha/dis}}$ represents the charge/discharge losses cost of ESS, c_{con} represents the cost of reactive operation in the converters, c_r represents the cost of line losses.

2) Constraint

The MDN power flow relationship is constrained by (9). For all types of converters, the constraints shown in (10)-(11) need to be satisfied, for GFM converters, the constraints shown in (12)-(13) need to be additionally satisfied, for ESS converters, the constraints shown in (14)-(15) need to be satisfied. For MCRs, the constraint shown in (16) needs to be satisfied.

Considering that the active power output of GFL converters operates in MPPT mode, the adjustable resources should smooth out the fluctuations of GFL converters:

$$\sum \Delta P_{\text{GFL}} + \sum \Delta P_{\text{GFM}} + \sum \Delta P_{\text{Load}} = 0 \tag{18}$$

Each node in MDN needs to satisfy the node voltage constraint:

$$0.96 |U_{\text{nom}}| \le |U| \le 1.06 |U_{\text{nom}}| \tag{19}$$

Where, U_{nom} is the nominal bus voltage For buses on distribution feeders, under the assumption that reverse power flow is not considered, it follows from (4) that b_2<0, Consequently, the voltage magnitude at any feeder bus should not exceed that at the head-end bus.

IV. Case Study

The proposed methods are evaluated on a practical MDN case which contains 19 substations in Hangzhou, China. The basic grid structure is shown in Fig. 2. All the methods are implemented in MATLAB R2024a and Simulink platform on a PC with 32 GB RAM and a 3.5GHz CPU.

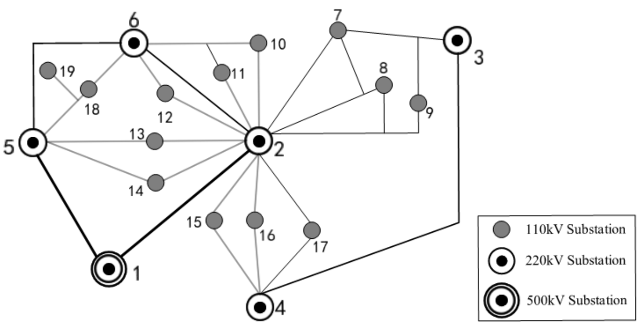

Figure 2. Grid Structure of This Case

A. *Distribution Network Equivalent Method*

To verify the effectiveness of the proposed distribution network equivalent method, we compared it with a traditional approach that (i) aggregates nominal loads by summation and (ii) computes an equivalent CVR_f as the load-weighted average of feeder CVR_f values. We tested it briefly on IEEE 33 bus system with different feeder CVR_f. The value of ZIP factors is shown in TABLE I.

TABLE I. ZIP Factos of Feeders in IEEE 33-Bus System

Feeders	ZIP Factors (%)			Type
	Z	*I*	*P*	
F1(2~18)	30	40	30	Mixed
F2(19~22)	50	25	25	Residential
F3(23~25)	30	50	20	Commercial
F4(26~33)	5	5	90	Industrial

The value of equivalent load under different methods is shown in TABLE II. The proposed method inherently captures feeder losses and mixed ZIP load behaviors in the equivalent model, leading to more accurate CVR response estimation. The error of the traditional method comes from both line losses and node voltages. In this system with low node voltages, the traditional method tends to overestimate power due to voltage deviations. But ignoring line losses causes an underestimation, which make these opposite effects largely cancel out. Therefore, in systems where node voltages are higher, these two errors will reinforce each other, producing significantly larger deviations from the actual system. In that case, the proposed method will have better performance because it takes into account line losses.

TABLE II. The Value of Equivalent Load With Different Method

Methods	Nominal Load (kW)	CVR_f	ΔP (kW)	ΔCVR_f
Traditional	3715	0.839	+46	-0.058
Proposed	3681	0.867	+12	-0.030
Exact	3669	0.897	/	/

B. *MDN Control Model*

We consider the low-voltage side of 110-kV substations to be the upstream boundary of the distribution network, while the low-voltage side of 220-kV substations is designated as the installation point for MCR. The integration points and capacity of the distributed RESs are summarized in Table III.

TABLE III. The Integration Points And Capacity of The RESs

Node	Type	Capacity (MVA)
7	GFL PV	3.57
9	GFM PV	0.82
10	ESS	1.20
11	GFM PV	5.57
12	GFL PV	5.57
15	ESS	0.93
19	GFL PV	1.60

We evaluate two scenarios where the GFL PV output increases and decreases by 10%, respectively. The result of active power and voltage optimization are shown in Fig. 3 (+10%) and Fig. 4 (-10%). In the increase scenario, ESS and load mainly support active power balancing while PV curtailment is avoided due to the imposed penalty. In the decrease scenario, GFM PV is more economical for active support while reactive resources contribute more to voltage regulation than load regulation.

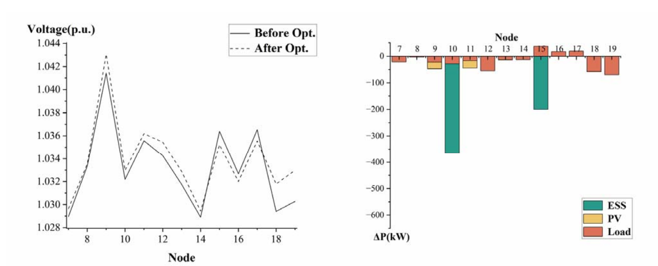

(a) Voltage (b) Active Power

Figure 3. The active power and voltage responses of +10% scenario

979-8-3315-8138-1

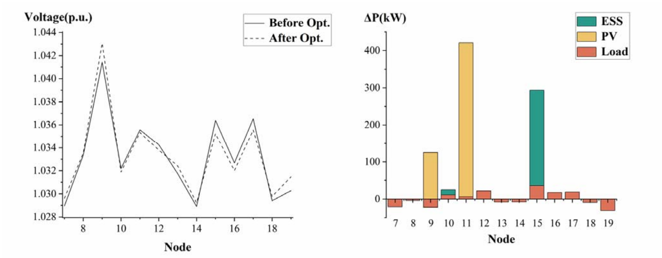

(a) Voltage (b) Active Power

Figure 4. The active power and voltage responses of -10% scenario

We also evaluate these scenarios without voltage-sensitive load control (but loads are still voltage-sensitive) and compare its economy. The C_{eco} is shown in the TABLE IV.

TABLE IV. THE ECONOMY WITH DIFFERENT CONTROL METHOD

Scenarios		C_1	C_2	C_3	C_4	C_{eco}
+10%	apply load control	5.10	15.04	12.30	13.54	45.98
	without load control	6.14	16.49	12.31	13.87	48.81
-10%	apply load control	0	10.60	12.11	13.56	36.27
	without load control	0	11.21	12.33	13.55	37.09

Where, C_1~C_4 represent four parts of C_{eco}. TABLE IV shows that the optimization model considering the voltage-sensitive load is more economy. The PV and ESS cost without voltage-sensitive load control is higher. Besides, voltage-sensitive load can also help to adjust the reactive power in the MDN, decrease the cost of Var/Volt optimization.

The ability of voltage regulation is also tested. We choose a high voltage scenario in the nighttime with light load and 0 PV output. The voltage optimization result is shown in Fig. 5.

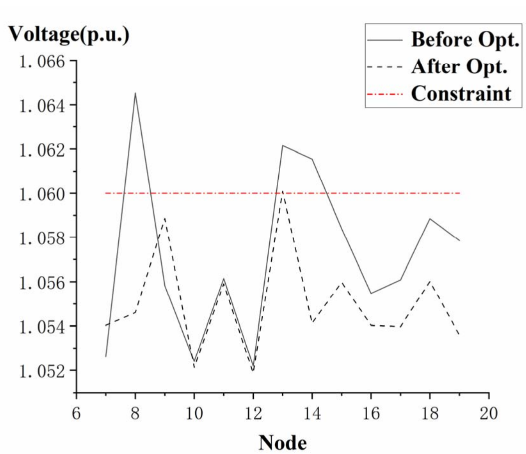

Figure 5. The voltage response of high voltage scenario

Overvoltage is eliminated and reactive-regulation costs are reduced, confirming the proposed model's effectiveness for high-voltage MDN operation.

V. CONCLUSION

This paper proposes an MDN calculation and control method based on voltage-sensitive load to reduce operating cost and improve renewable energy utilization. Based on the case studies, the following conclusions are drawn:

(1) The proposed aggregation and MDN calculation framework accurately represents embedded ZIP characteristics and losses of distribution networks at the MDN scale, enabling consistent power–voltage evaluation across MDN.

(2) Coordinated dispatch of voltage-sensitive loads in MDNs maintains voltage compliance and reduces total operating cost under different operating scenarios.

REFERENCES

[1] G. Notton, M. L. Nivet, C. Voyant *et al.*, "Intermittent and stochastic character of renewable energy sources: Consequences, cost of intermittence and benefit of forecasting," *Renew. Sust. Energ. Rev.*, vol. 87, pp. 96-105, May 2018.

[2] P. Yu, H. Zhang, Z Hu, and Y. Song, "Voltage control of distribution grid with district cooling systems based on scenario-classified reinforcement learning," *Appl. Energ.*, vol. 377(B), pp. 124415, Jan. 2025.

[3] X. Ding, S. Liao, J. Xu and Y. Sun, "A source-load coordinated control strategy in an industrial aluminum production microgrid for smoothing wind power fluctuations," in *Proc. 2023 IEEE/IAS Industrial and Commercial Power System Asia*, pp. 1076-1081.

[4] J. Xu, B. Xie, S. Liao, *et al.*, "CVR-Based real-time power fluctuation smoothing control for distribution systems with high penetration of PV and experimental demonstration," *IEEE Trans. Smart Grid*, vol. 13, no. 5, pp. 3619-3635, Sept. 2022.

[6] *IEEE Standard for Conservation Voltage Reduction (CVR) Data Collection and Management Procedures*, IEEE Std. 3102-2024, Jan. 2025.

[7] G. De Carne, G. Buticchi, M. Liserre and C. Vournas, "Real-Time primary frequency regulation using load power control by smart transformers," *IEEE Trans. Smart Grid*, vol. 10, no. 5, pp. 5630-5639, Sept. 2019.

[8] B. Alghamdi and C. A. Cañizares, "Frequency regulation in isolated microgrids through optimal droop gain and voltage control," *IEEE Trans. Smart Grid*, vol. 12, no. 2, pp. 988-998, March 2021.

[9] A. Garces, "A linear three-phase load flow for power distribution systems," *IEEE Trans. Power Syst.*, vol. 31, no. 1, pp. 827-828, Jan. 2016.

[10] Q. Zhang, F. Bu, Y. Guo and Z. Wang, "Tractable data enriched distributionally robust chance-constrained conservation voltage reduction," *IEEE Trans. Power Syst.*, vol. 39, no. 1, pp. 821-835, Jan. 2024.

[11] I. Džafić, R. A. Jabr and T. Hrnjić, "High performance distribution network power flow using wirtinger calculus," *IEEE Trans. Smart Grid*, vol. 10, no. 3, pp. 3311-3319, May 2019.

[12] J. Wei, Q. Huang, L. Liu, P. Wang and P. Zhou, "MSVC based multi-side coordinated reactive compensation capacity configuration and voltage/var control in substation," in *Proc. 2014 9th IEEE Conference on Industrial Electronics and Applications*, pp. 596-602.

[13] K. Feng, J. Wang, G. Guo, *et al.*, "Research on Multi-Mode Control Strategy of Distributed Static Synchronous Series Compensator," in *Proc. 2023 4th International Conference on Power Engineering*, pp. 341-346.

979-8-3315-8138-1